JOURNAL OF THERMOPHYSICS AND HEAT TRANSFER
Vol. 8, No. 4, Oct.–Dec. 1994

Laminar Mixed Convection from a Circular Cylinder Using a Body-Fitted Coordinate System

Cha'o-Kuang Chen,* Yue-Tzu Yang,† and Sang-Ru Wu‡
National Cheng Kung University, Tainan, Taiwan, Republic of China

A numerical investigation of laminar mixed convection from a horizontal isothermal cylinder is presented. The governing equations in terms of the stream function, vorticity and temperature are expressed in a body-fitted coordinate system and solved numerically by the spline alternating direction implicit method. Results are presented for Reynolds number Re from 20 to 100 with Grashof numbers up to $Gr = 5Re^2$. The Prandtl number was kept at a constant value of 0.7. Results are presented for the streamlines, velocity vectors, and isotherms as well as the local and average Nusselt number at different values of the Reynolds number and Grashof number. Comparison with previous experimental results shows good agreement.

Nomenclature

Gr = Grashof number, $g\beta(T_s - T_\infty)(2R)^3/\nu^2$
h = convective heat transfer coefficient
J = Jacobian
k = thermal conductivity
$\underline{Nu}$ = local Nusselt number, $2Rh/k$
$\overline{Nu}$ = average Nusselt number
P = coordinate control function
Pr = Prandtl number
p = pressure
Q = coordinate control function
R = radius of cylinder
Re = Reynolds number, $2RU_\infty/\nu$
r = radial coordinate
T = temperature
T_s = surface temperature
T_∞ = freestream temperature
t = time
U_∞ = freestream velocity
u = x-velocity component
v = y-velocity component
x = x coordinate
y = y coordinate
β = thermal coefficient of expansion
Γ = boundary in the physical plane
Γ^* = boundary in the transformed plane
η, ξ = dimensionless transformed coordinates
θ = plane angle
ν = kinematic viscosity
ρ = density of fluid
ψ = stream function
ω = vorticity

Introduction

HEAT transfer from a horizontal cylinder has been studied experimentally and theoretically because of its numerous engineering applications. The first comprehensive experimental work on the effect of various parameters on the rate of heat transfer from a circular cylinder was carried out by Hatton et al.[1] In their work, heat transfer measurements were performed for Reynolds numbers up to 45 and Rayleigh numbers up to 10. The effect of freestream direction on the heat transfer process was also investigated by Hatton et al. Gebhart and Pera[2] studied the same problem for various Prandtl numbers, but restricted their study to very small Reynolds numbers. Sharma and Sukhatme[3] investigated the phenomenon experimentally for high Reynolds and Grashof numbers (Re up to 5×10^3, and Gr up to 7×10^3). Criteria for transition from free to combined to forced convection were suggested. The influence of flow direction on combined heat convection from a horizontal cylinder to air was studied experimentally by Oosthuizen and Madan.[4]

Although many experimental studies have been performed, it seems that theoretical studies are relatively rare, and most of them have been limited to the boundary-layer type. The problem of cross-mixed convection from a horizontal circular cylinder was investigated by Badr[5] with Reynolds number $1 < Re < 40$ and Grashof numbers up to $Gr/(Re^2) = 5$. His study was based on the solution of the full Navier-Stokes and energy equations for two-dimensional flow. The details of the steady velocity and thermal boundary layers were obtained and accordingly the variation of vorticity, pressure, and local Nusselt number around the cylinder surface were also plotted. Jain and Lohar[6] have treated the unsteady mixed convection about a circular cylinder with $Re = 100$ and 200. However, their flow was restricted to the transient state only ($t \leq 20$). Armaly et al.[7] prescribed the correlation equations for mixed convection flow across horizontal cylinders and spheres in air.

In this work, the problem of mixed convection from a horizontal isothermal cylinder is considered. The forced flow is assumed to be perpendicular to the direction of free convection. The Navier-Stokes equations and the energy equation for an unsteady incompressible fluid flow are solved by the use of a body-fitted coordinate system and the spline alternating direction implicit (SADI) method.[8–11] Results are presented for Reynolds numbers from 20 to 100, with Grashof numbers up to $Gr = 5Re^2$. The Prandtl number was kept at a constant value of 0.7. For flows around bluff geometries with flow separation, the finite difference method, or the finite element method are found to be inadequate. It needs a lot of grid and computer time to calculate the logarithmic transformation of the radial coordinate. It may lead to poor application of the boundary condition by using the interpolation between grid points to represent boundary condition on a curved boundary. It also needs a finer element or grid size to calculate large gradient accurately near the wall. Therefore, it takes a large amount of computer storage and computational time. With the above reason, this article prescribes a transformation of the physical flowfield for arbitrary geometry to

Received Sept. 15, 1993; revision received Feb. 9, 1994; accepted for publication Feb. 10, 1994.
*Professor, Department of Mechanical Engineering.
†Associate Professor, Department of Mechanical Engineering.
‡Graduate Student, Department of Mechanical Engineering.

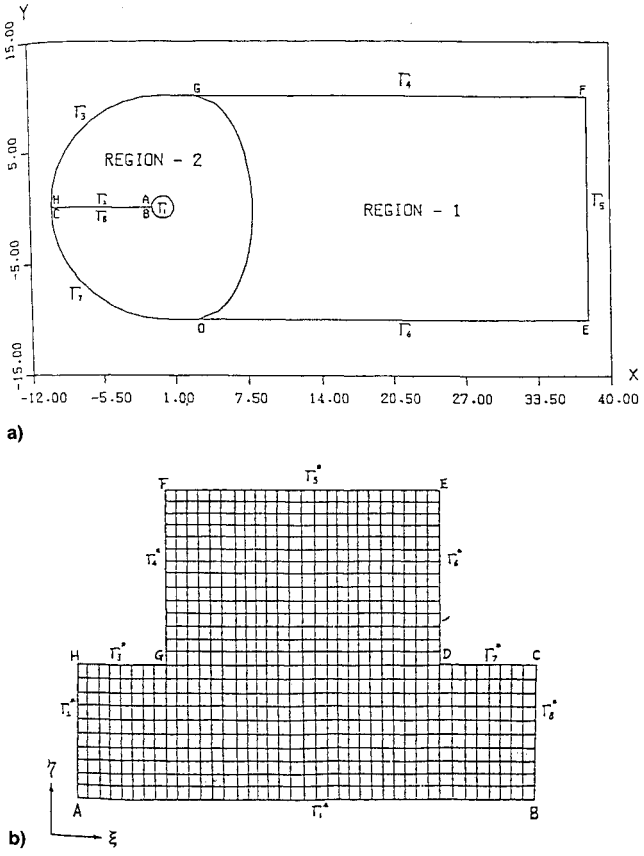

Fig. 1 Transformation of the solution domain: a) physical and b) transformed plane.

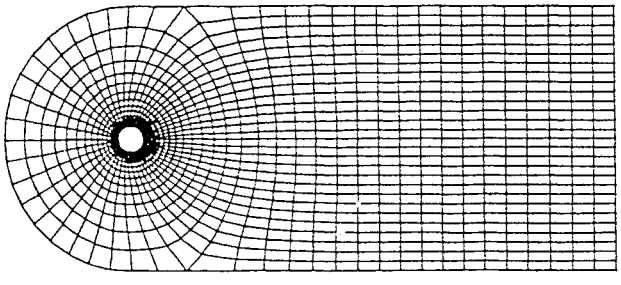

Fig. 2 Body-fitted coordinate system.

a rectangular computational domain with coordinate lines coinciding with all boundaries of the flow region.

Mathematical Formulation

Consider the problem of R and an isothermal surface with T_s, placed in a uniform T_∞ and velocity U. The forced flow is assumed to be perpendicular to the direction of free convection. The effect of temperature variation on fluid properties is assumed negligible and the fluid is incompressible. The cylinder's end effects on the velocity and temperature field are neglected and accordingly the flow is assumed two dimensional. The transformation of the solution domain is shown in Fig. 1. Figure 1a presents the computational domain in the physical plane, whereas Fig. 1b shows the proposed boundaries of the flow domain in the transformed plane. The dimensionless governing equations can be written as follows:

energy equation

$$\frac{\partial T}{\partial t} + \frac{\partial \psi}{\partial y}\frac{\partial T}{\partial x} - \frac{\partial \psi}{\partial x}\frac{\partial T}{\partial y} = \frac{2}{RePr}\left(\frac{\partial^2 T}{\partial x^2} + \frac{\partial^2 T}{\partial y^2}\right) \tag{1}$$

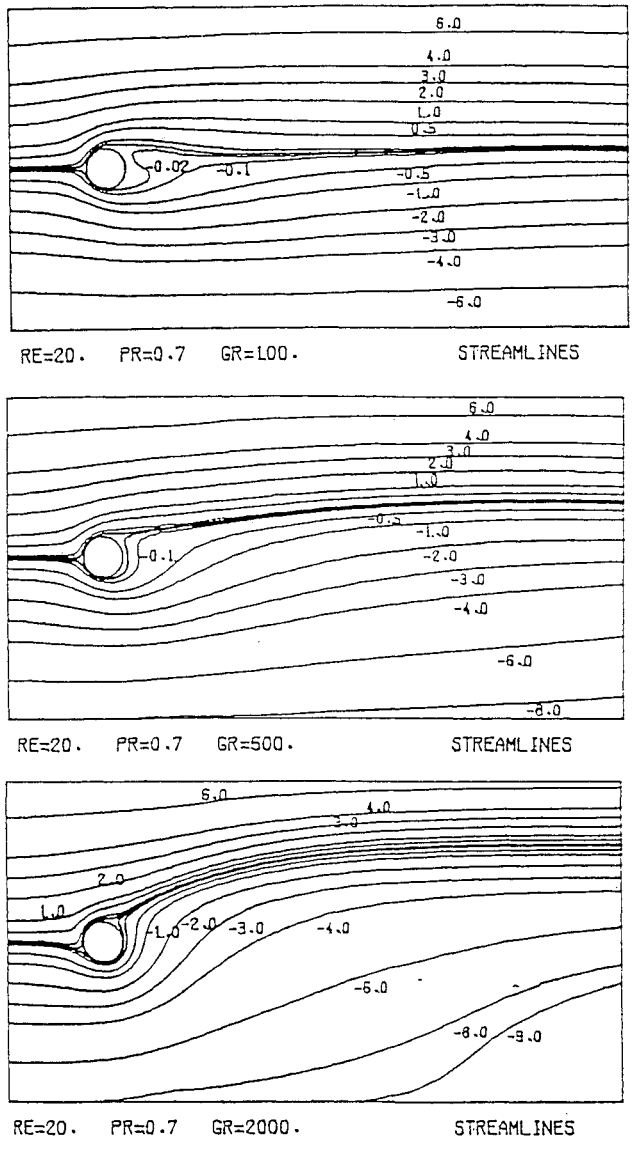

Fig. 3 Steady-state streamline patterns for different values of Gr at $Re = 20$.

vorticity equation

$$\frac{\partial \omega}{\partial t} + \frac{\partial \psi}{\partial y}\frac{\partial \omega}{\partial x} - \frac{\partial \psi}{\partial x}\frac{\partial \omega}{\partial y} = \frac{2}{Re}\left(\frac{\partial^2 \omega}{\partial x^2} + \frac{\partial^2 \omega}{\partial y^2}\right) + \frac{Gr}{2Re^2}\frac{\partial T}{\partial x} \tag{2}$$

stream function equation

$$\frac{\partial^2 \psi}{\partial x^2} + \frac{\partial^2 \psi}{\partial y^2} = -\omega \tag{3}$$

The above equations have been written in terms of the following dimensionless quantities:

$$x^* = \frac{x}{R}, \quad y^* = \frac{y}{R}, \quad r^* = \frac{r}{R}, \quad u^* = \frac{u}{U}$$

$$v^* = \frac{v}{U}, \quad p^* = \frac{p}{\rho U^2}, \quad \omega^* = \frac{\omega R}{U} \tag{4}$$

$$\psi^* = \frac{\psi}{UR}, \quad T^* = \frac{T - T_\infty}{T_s - T_\infty}, \quad t^* = \frac{tU}{R}$$

In the following the notation * is omitted for convenience.

The dimensionless initial conditions are

$$\psi = 0, \quad \omega = 0, \quad T = 0 \tag{5}$$

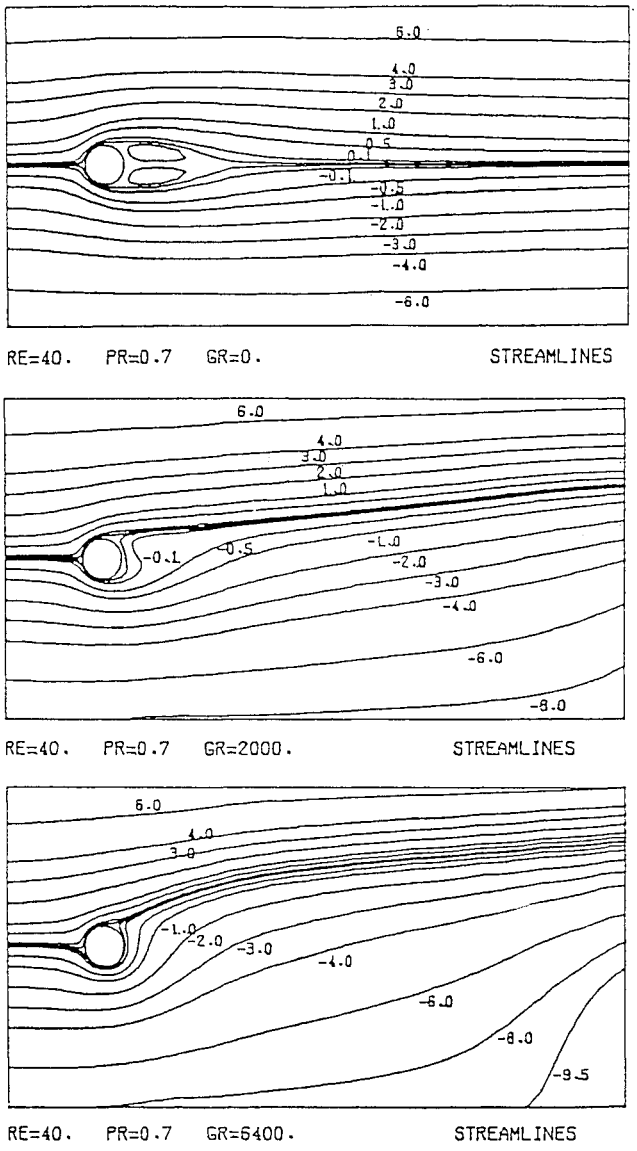

Fig. 4 Steady-state streamline patterns for different values of *Gr* at *Re* = 40.

The boundary conditions on the cylinder are

on the boundary Γ_1

$$T = 1, \qquad \psi = 0, \qquad \omega = -\nabla^2\psi \tag{6}$$

on the boundaries Γ_3, Γ_4, Γ_6, and Γ_7

$$T = 0, \qquad \psi = [r - (1/r)] \sin\theta, \qquad \omega = 0 \tag{7}$$

on the boundary Γ_5

$$\frac{\partial T}{\partial x} = 0, \qquad \frac{\partial \psi}{\partial x} = 0, \qquad \frac{\partial \omega}{\partial x} = 0 \tag{8}$$

Numerical Procedure

The governing equations, initial, and boundary conditions can be expressed in body-fitted coordinates. The boundary-fitted physical coordinate system is created using the method of Thompson et al.[12–15] The domain of solution considered in this study extended to a downstream distance of approximately $38R$ from the center of the cylinder, and to an upstream distance of $10R$. In order to create grid lines conveniently, the whole computational domain was divided into two subregions, region-1 and region-2. In Fig. 1, region-1 is a

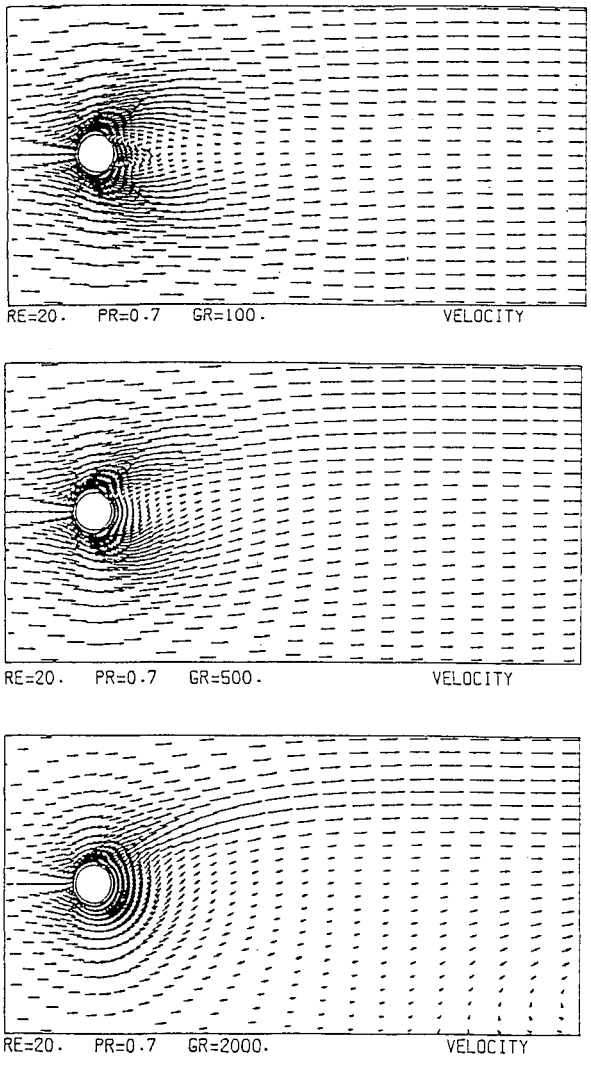

Fig. 5 Effect of *Gr* on the steady velocity pattern at *Re* = 20.

simply connected region, and region-2 is a multiple connected region around the cylinder. The curve GD is the interface of the two subregions. It was assumed to satisfy the elliptical curve

$$\frac{(x - b)^2}{a^2} + \frac{y^2}{10^2} = 1 \tag{9}$$

where $a = 5$, $b = 3$.

In this method, the following system of Poisson equations must be solved:

$$\xi_{xx} + \xi_{yy} = P(\xi, \eta) \tag{10a}$$

$$\eta_{xx} + \eta_{yy} = Q(\xi, \eta) \tag{10b}$$

Where P and Q are the coordinate control functions that provide the control of the mesh distribution. Since it is desired to perform all numerical calculations in the transformed plane, the dependent and independent variables must be interchanged in Eqs. (10a) and (10b). The transformed equations are

$$\alpha x_{\xi\xi} - 2\beta x_{\xi\eta} + \gamma x_{\eta\eta} = -J^2(Px_\xi + Qx_\eta) \tag{11a}$$

$$\alpha y_{\xi\xi} - 2\beta y_{\xi\eta} + \gamma y_{\eta\eta} = -J^2(Py_\xi + Qy_\eta) \tag{11b}$$

where

$$\alpha = x_\eta^2 + y_\eta^2, \qquad \beta = x_\xi x_\eta + y_\xi y_\eta, \qquad \gamma = x_\xi^2 + y_\xi^2$$

$$J = \frac{\partial(x, y)}{\partial(\xi, \eta)} = x_\xi y_\eta - x_\eta y_\xi \neq 0$$

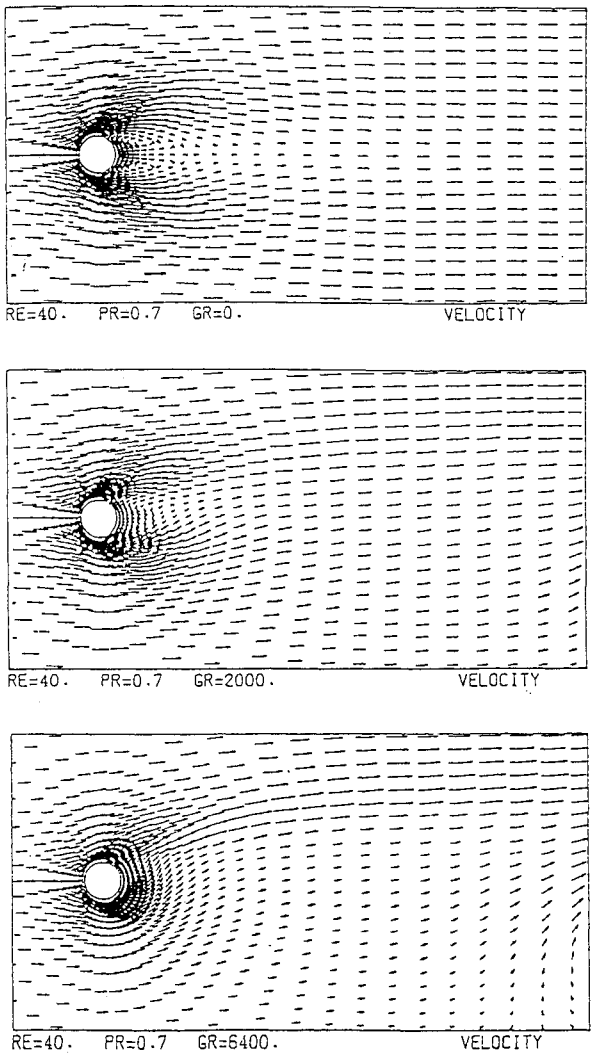

Fig. 6 Effect of *Gr* on the steady velocity pattern at *Re* = 40.

The difficulty of interior grid control has been overcome by devising general source terms P and Q that are computed from the Dirichlet boundary values. The source terms have the form

$$P = \bar{\phi}(\xi, \eta)(\xi_x^2 + \xi_y^2)$$
$$Q = \bar{\psi}(\xi, \eta)(\eta_x^2 + \eta_y^2) \tag{12}$$

where the parameters $\bar{\phi}$, $\bar{\psi}$ are yet to be specified. Based on introducing these terms, Eqs. (11a) and (11b) assume the form

$$\alpha(x_{\xi\xi} + \bar{\phi}x_\xi) - 2\beta x_{\xi\eta} + \gamma(x_{\eta\eta} + \bar{\psi}x_\eta) = 0$$
$$\alpha(y_{\xi\xi} + \bar{\phi}y_\xi) - 2\beta y_{\xi\eta} + \gamma(y_{\eta\eta} + \bar{\psi}y_\eta) = 0 \tag{13}$$

It is clearly shown that Eqs. (13) possesses exponential solutions if the parameters $\bar{\phi}$, $\bar{\psi}$ are locally constant. If a set of boundary values (x, y) on the boundary of the computational domain is given, one can determine the parameters by requiring that the given boundary values satisfy appropriate limiting forms of Eqs. (13) along the boundary of the computational domain.

The transformed Eq. (11) was solved with the successive over relaxation (SOR) method. Once a grid is generated, the values of the coefficients α, β, γ, and J are evaluated and stored for use in the solution of the governing equations.

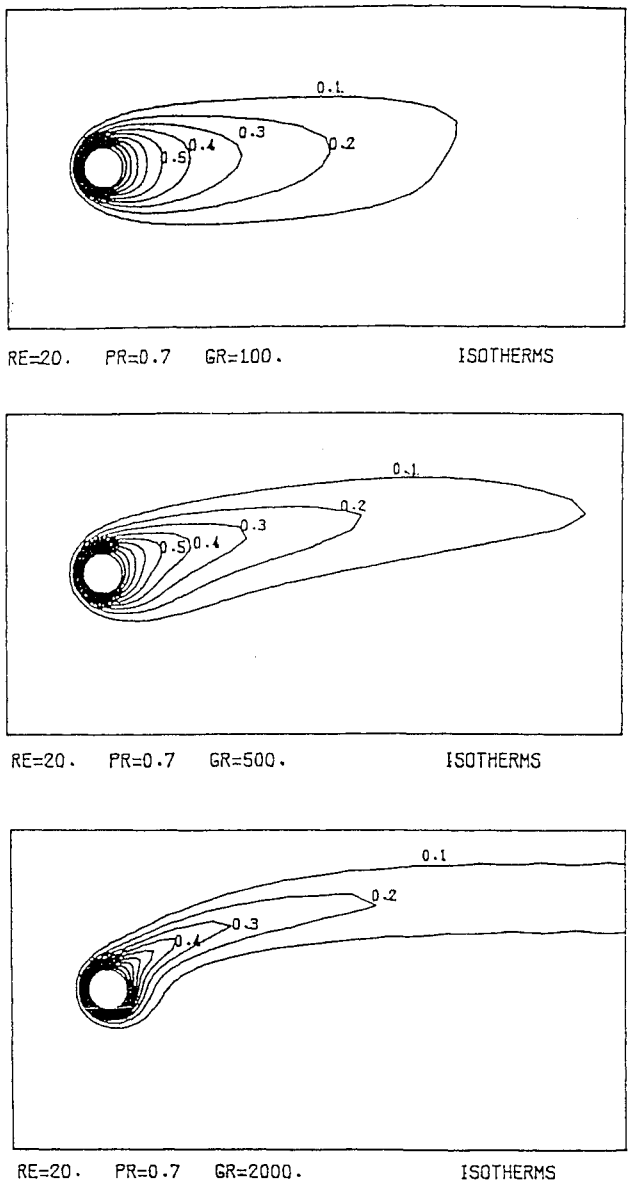

Fig. 7 Steady-state isotherms for different values of *Gr* at *Re* = 20.

The governing Eqs. (1–3) in terms of the transformed coordinates are

$$T_t + (1/J)(\psi_\eta T_\xi - \psi_\xi T_\eta) = (2/RePr)[(1/J^2)(\alpha T_{\xi\xi} + \gamma T_{\eta\eta}) + P(\xi, \eta)T_\xi + Q(\xi, \eta)T_\eta] \tag{14}$$

$$\omega_t + (1/J)(\psi_\eta \omega_\xi - \psi_\xi \omega_\eta) = (2/Re)[(1/J^2)(\alpha\omega_{\xi\xi} + \gamma\omega_{\eta\eta}) + P(\xi, \eta)\omega_\xi + Q(\xi, \eta)\omega_\eta] \tag{15}$$

$$(1/J^2)(\alpha\psi_{\xi\xi} + \gamma\psi_{\eta\eta}) + P(\xi, \eta)\psi_\xi + Q(\xi, \eta)\psi_\eta = -\omega \tag{16}$$

where

$$\alpha = x_\eta^2 + y_\eta^2, \qquad \gamma = x_\xi^2 + y_\xi^2$$

$$P(\xi, \eta) = \bar{\phi}(\xi, \eta)(\alpha/J^2), \qquad Q(\xi, \eta) = \bar{\psi}(\xi, \eta)(\gamma/J^2)$$

In terms of the transformed coordinates, the initial conditions become

$$\psi = 0, \qquad \omega = 0, \qquad T = 0 \tag{17}$$

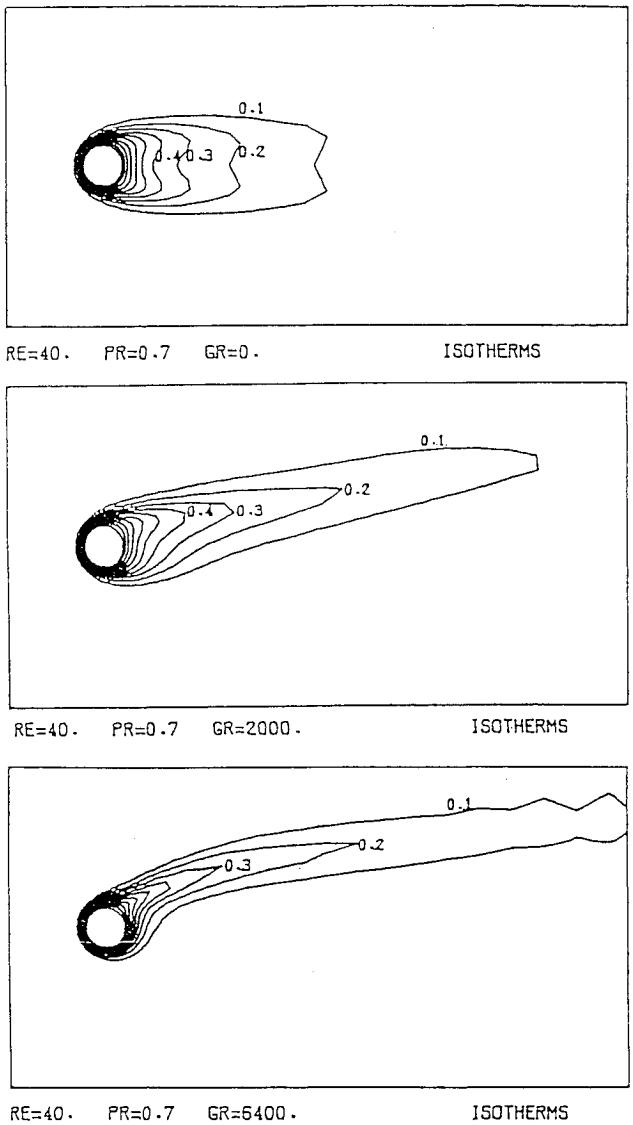

Fig. 8 Steady-state isotherms for different values of *Gr* at *Re* = 40.

on the boundary Γ_1^*

$$T = 1, \quad \psi(\xi, 1, t) = 0, \quad \psi_\eta = \psi_\xi = 0$$
$$\omega(\xi, 1, t) = -(1/J^2)(\alpha\psi_{\xi\xi} + \gamma\psi_{\eta\eta}) \tag{18}$$

on the boundaries Γ_3^*, Γ_4^*, Γ_6^*, and Γ_7^*

$$T(\xi, \eta, t) = 0, \quad \omega(\xi, \eta, t) = 0$$
$$(\xi, \eta, t) = [r - (1/r)]\sin\theta$$
$$\psi_\xi = uy_\xi - vx_\xi, \quad \psi_\eta = uy_\eta - vx_\eta \tag{19}$$

on the boundary Γ_5^*

$$T_\eta = 0, \quad \psi_\eta = 0, \quad \omega_\eta = 0 \tag{20}$$

The transformed governing equations and boundary conditions were discretized by using the cubic spline collocation formulation.[8] The SADI procedure was applied to perform the numerical computation. The calculation solutions appear to be independent of grid distribution of 51 × 33, and the spatial grid resolution was set as $\Delta\xi = \Delta\eta = 1$ as shown in Fig. 2. To obtain a reasonably accurate solution small time steps are reduced to the order of $\frac{1}{2}Re$ in the initial phase to resolve the motion of the fluid. Time steps were subsequently increased to values of $1/Re$ or $2/Re$ without significant in-

Table 1 Comparisons of average Nusselt number

Re	*Gr*	Gr/Re^2	Present work, $\overline{Nu}$	Badr,[5] $\overline{Nu}$
20	0	0.0	2.5806	2.54
	100	0.25	2.5873	2.52
	500	1.25	2.690	2.65
	1000	2.5	2.911	2.85
	2000	5.0	3.240	3.10
40	0	0.0	3.470	3.48
	400	0.25	3.481	3.49
	2000	1.25	3.583	3.60
	3200	2.0	3.780	3.76
	6400	4.0	4.228	4.17

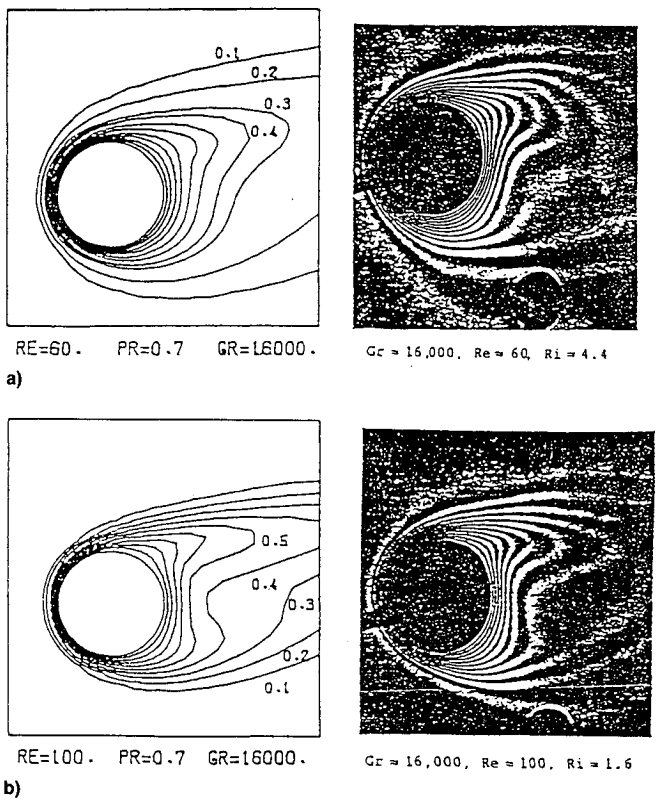

Fig. 9 Comparison of the steady-state isotherms between the interferometer photograph of Krause and Tarasuk[16] and the present results.

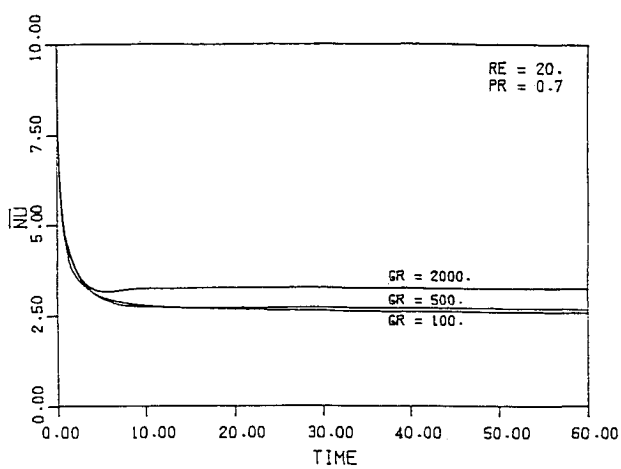

Fig. 10 Variation of $\overline{Nu}$ with time for different values of *Gr* at *Re* = 20.

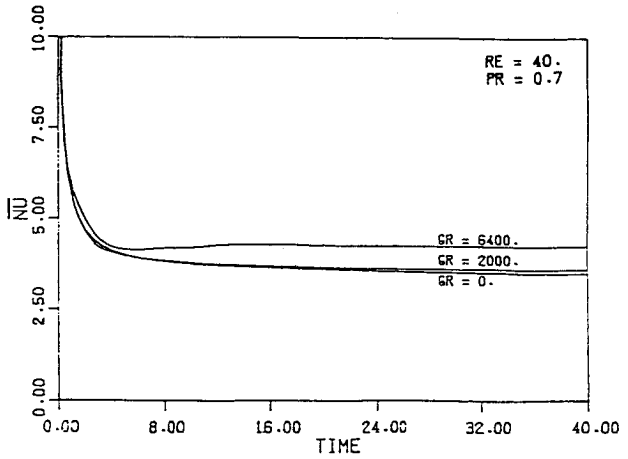

Fig. 11 Variation of $\overline{Nu}$ with time for different values of Gr at $Re = 40$.

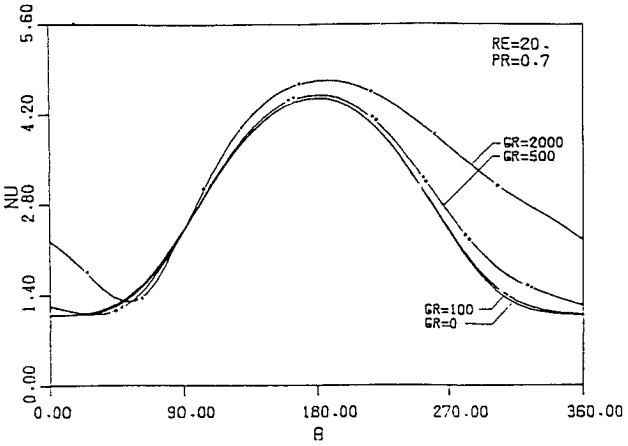

Fig. 12 Variation of the steady Nu around the cylinder surface for different values of Gr at $Re = 20$.

creases in the number of iterations required to converge each step.

The convergence criteria for the stream function, vorticity, and temperature were

$$\frac{\max_{i,j}|\psi_{i,j}^{s+1} - \psi_{i,j}^{s}|}{\max_{i,j}|\psi_{i,j}^{s+1}|} \leq 10^{-4} \tag{21}$$

$$\frac{\max_{i,j}|\omega_{i,j}^{k+1} - \omega_{i,j}^{k}|}{\max_{i,j}|\omega_{i,j}^{k+1}|} \leq 10^{-4} \tag{22}$$

$$\frac{\max_{i,j}|T_{i,j}^{k+1} - T_{i,j}^{k}|}{\max_{i,j}|T_{i,j}^{k+1}|} \leq 10^{-4} \tag{23}$$

where s and k are the iteration number. After convergence of the numerical solution has been achieved, the local and the average Nusselt numbers can be calculated as

$$Nu = (2Rh/k) \tag{24}$$

$$\overline{Nu} = \frac{1}{2\pi}\int_0^{2\pi} Nu \, d\theta \tag{25}$$

Results and Discussion

Figures 3 and 4 show the streamline patterns when $Re = 20$ and 40 for different values of Gr. It is clear from these figures that the rear stagnation point and reattachment point move upward significantly with the increase of Gr/Re^2. This is mainly because the buoyant forces are aiding the acceleration of flow downstream of the cylinder.

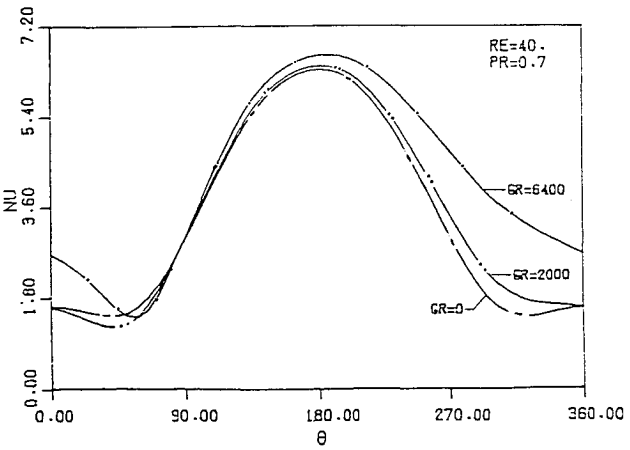

Fig. 13 Variation of the steady Nu around the cylinder surface for different values of Gr at $Re = 40$.

The effect of Gr on the velocity field is presented in Figs. 5 and 6. It can be seen from these figures that the reverse flow in the wake of the cylinder is strongly influenced by the ratio Gr/Re^2. It is also seen that there is no reverse flow taking place at large values of Gr/Re^2, and the vortices completely disappear.

The isotherms for different values of Gr are given in Figs. 7 and 8. It can be seen that the temperature field is almost symmetrical at small values of Gr. With the increase of Gr the point of separation moves upward and the isothermal pattern changes accordingly.

In Figs. 9a and 9b the computed isotherms are compared with the interferometer photograph of Krause and Tarasuk[16] for $Gr = 16{,}000$ and $Re = 60$ and 100. The agreement is good.

The variation of $\overline{Nu}$ with time is shown in Figs. 10 and 11. When $Re = 20$ and 40 for different values of Gr, with the increase of the thermal boundary layer and the $\overline{Nu}$ decreases accordingly. The average Nusselt numbers obtained in the present work are in good agreement with the results of Badr[5] as shown in Table 1. The large difference occurs at high Gr within 4.5%.

The variation of Nu around the cylinder surface is shown in Figs. 12 and 13 for $Re = 20$ and 40, respectively. For forced convection case ($Gr = 0$) Nu is maximum at $\theta = 180$ deg, and Nu is minimum at $\theta = 0$ deg. With the increase of Gr the maximum value of Nu continues to occur near $\theta = 180$ deg, and the point of minimum Nu moves upward towards $\theta = 90$ deg. It is also seen that increasing Gr tends to increase Nu.

Conclusions

A numerical solution has been obtained for the problem of cross-mixed convection from a circular cylinder. The governing equations expressed in the body-fitted coordinates were solved numerically by the SADI method. Good agreement was found with experimental data. The streamline and isotherm patterns are presented to show the details of the velocity and temperature fields. The method is confirmed to apply successfully to the problem of cross-mixed convection.

References

[1]Hatton, A. P., James, D. D., and Swire, H. W., "Combined Forced and Natural Convection with Low-Speed Air Flow over Horizontal Cylinders," *Journal of Fluid Mechanics*, Vol. 42, June 1970,

pp. 17–31.

[2]Gebhart, B., and Pera, L., "Mixed Convection for Long Horizontal Cylinders," *Journal of Fluid Mechanics*, Vol. 45, Jan. 1970, pp. 49–64.

[3]Sharma, G. K., and Sukhatms, S. P., "Combined Free and Forced Convection Heat Transfer from a Heated Tube to a Transverse Air Stream," *Journal of Heat Transfer*, Vol. 91, No. 3, 1969, pp. 457–459.

[4]Oosthuizen, P. H., and Madan, S., "The Effect of Flow Direction on Combined Convective Heat Transfer from Cylinders to Air," *Journal of Heat Transfer*, Vol. 93, No. 2, 1971, pp. 240–242.

[5]Badr, H. M., "A Theoretical Study of Laminar Mixed Convection from a Horizontal Cylinder in a Cross Stream," *Journal of Heat and Mass Transfer*, Vol. 26, No. 5, 1983, pp. 639–653.

[6]Jain, P. C., and Lohar, B. L., "Unsteady Mixed Convection Heat Transfer from a Horizontal Circular Cylinder," *Transactions of the American Society of Mechanical Engineers, Journal of Heat Transfer*, Vol. 101, No. 1, 1979, pp. 126–131.

[7]Armaly, B. F., Chen, T. S., and Ramachandran, N., "Correlations for Mixed Convection Flow Across Horizontal Cylinders and Spheres," *Transactions of the American Society of Mechanical Engineers, Journal of Heat Transfer*, Vol. 110, No. 2, 1988, pp. 511–514.

[8]Rubin, S. G., and Graves, R. A., "Viscous Flow Solution with a Cubic Spline Approximation," *Computers and Fluids*, Vol. 3, No. 1, 1975, pp. 1–36.

[9]Rubin, S. G., and Khosla, P. K., "Higher-Order Numerical Solution Using Cubic Splines," *AIAA Journal*, Vol. 14, No. 7, 1976, pp. 851–858.

[10]Rubin, S. G., and Khosla, P. K., "Polynomial Interpolation Methods for Viscous Flow Calculations," *Journal of Computational Physics*, Vol. 24, No. 3, 1977, pp. 217–244.

[11]Wang, P., and Kahawita, R., "Numerical Integration of Partial Differental Equations Using Cubic Splines," *International Journal of Computer Mathematics*, Vol. 13, No. 3, 1983, pp. 271–286.

[12]Thompson, J. F., Thames, F. C., Mastin, C. W., and Shanks, S. P., "Use of Numerically Generated Body-Fitted Coordinate Systems for Solution of the Navier-Stokes Equations," *Proceedings of the AIAA 2nd Computational Fluid Dynamics Conference* (Hartford, CT), AIAA, New York, 1975.

[13]Thompson, J. F., Thames, F. C., and Mastin, C. W., "TOMCAT," *Journal of Computational Physics*, Vol. 24, No. 3, 1977, pp. 274–302.

[14]Thames, F. C., Thompson, J. F., Mastin, C. W., and Walker, R. L., "Numerical Solution for Viscous and Potential Flow About Arbitrary Two-Dimensional Bodies Using Body-Fitted Coordinate Systems," *Journal of Computational Physics*, Vol. 24, No. 3, 1977, pp. 254–273.

[15]Thompson, J. F., Thames, F. C., and Mastin, C. W., "Boundary-Fitted Curvilinear Coordinate System for Solution of Partial Differential Equations on Fields Containing any Number of Arbitrary Two-Dimensional Bodies," NASA CR-2729, 1976.

[16]Krause, J. R., and Tarasuk, J. D., "An Interferometric Study of Mixed Convection from a Horizontal Cylinder," *ASME HTD, Fundamentals of Forced and Mixed Convection*, Vol. 42, 1985, pp. 171–179.